Heliyon 10 (2024) e30749

Contents lists available at ScienceDirect

Heliyon

journal homepage: www.cell.com/heliyon

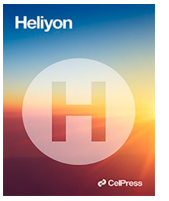

Research article

Identification and morphological characterization of different types of plastic microparticles

Dulce L. Soliz [a], Gema Paniagua González [c,*], Juan Muñoz-Arnanz [b], Juan Carlos Bravo-Yagüe [c], Pilar Fernández Hernando [c], Rosa María Garcinuño Martínez [c,**]

[a] Researcher in Training at the International Doctoral School of UNED, in the Doctoral Program in Sciences, Spain
[b] Department of Instrumental Analysis and Environmental Chemistry, Institute of Organic Chemistry (IQOG, CSIC), Juan de la Cierva 3, Madrid, 28006, Spain
[c] Department of Analytical Sciences, Faculty of Sciences, National University of Distance Education, UNED, Las Rozas, 28232, Madrid, Spain

ARTICLE INFO

Keywords:
Microplastics
Polymer identification SEM
FTIR-ATR spectroscopy light microscopy
staining dyes

ABSTRACT

The knowledge of the polymeric composition of microplastics (MPs) is interesting because offers useful information on the resistance, durability, and degradability of these materials, also allowing progress in the control of this contamination. However, there is currently a lack of reliable standardized methods for the identification, and characterization of the plastic microparticles. This work uses different techniques in a complementary manner for the identification, and characterization of MPs that more frequently are found in the environment. A total of 10 types of plastics were collected (polystyrene (PS), polyethylene terephthalate (PETE), polyethylene (PE), high- and low-density polyethylene (HDPE and LDPE, respectively), polyvinyl chloride (PVC), polypropylene (PP), polytetrafluoroethylene (PTFE), Polyamide (PA, Nylon 6,6) and poly-carbonate (PC)) and their chemical identification were analyzed by reflectance-attenuated infrared (FTIR-ATR). Furthermore, the samples were observed using light microscopy, and scan-ning electron microscopy (SEM). Also, staining with 12 different dyes was performed to improve the identification of microplastics. The results of this study revealed that PETE, PE, HDPE and LDPE, whose SEM images exhibited smoothness and flat uniformity of their surface, were not (or less) susceptible to adsorb staining solutions while PP, PA, PVC, and PTFE, were capable of adsorbing the dye solutions.

1. Introduction

Plastic materials are organic polymers derived from petroleum, which have different properties and characteristics such as durability, lightness, and versatility, besides their easy production and low cost [1].

The most used plastics are high- and low-density polyethylene (HDPE and LDPE, respectively), polyvinyl chloride (PVC),

* Corresponding author. Avda. Esparta s/n, Ctra. de Las Rozas-Madrid (M-505) Km. 5, 28232, Las Rozas Madrid, Spain.
** Corresponding author.
E-mail addresses: dsoliz@ccia.uned.es (D.L. Soliz), gpaniagua@ccia.uned.es (G. Paniagua González), juan.ma@iqog.csic.es (J. Muñoz-Arnanz), juancarlos.bravo@ccia.uned.es (J.C. Bravo-Yagüe), pfhernando@ccia.uned.es (P. Fernández Hernando), rmgarcinuno@ccia.uned.es (R.M. Garcinuño Martínez).

https://doi.org/10.1016/j.heliyon.2024.e30749
Received 27 January 2024; Received in revised form 30 April 2024; Accepted 3 May 2024
Available online 15 May 2024

polypropylene (PP), polyethylene terephthalate (PETE), polystyrene (PS) and polyurethane (PU) [2].

The excessive and growing manufacture of plastics has arranged the production of these materials in one of the great problems of the 21st century due to an accidental/indiscriminate discharges, inappropriate recycling, or incorrect handling. Therefore, plastic waste has accumulated uncontrollably in the various environmental compartments, affecting a wide range of aquatic and terrestrial ecosystems [3].

Once in the environment, plastics debris can breakdown by ultraviolet radiation, abrasion, heat, etc., forming small fragments called microplastics (MPs) with different colors, sizes, and shapes [4]. The US National Oceanographic and Atmospheric Agency (NOAA) held the first international meeting on microplastics in 2008, where polymeric particles with a size of less than 5 mm were established as microplastics [5].

As a result of their small size, these waste particles can persist for extended periods in soils and sediments, in the air, and in aquatic environments. MPs exposure on aquatic organism can cause, physical and physiological damage such as block the digestive organs, low growth rate, oxidative stress, decreased fecundity, etc. [6]. In addition, they can release their chemical additives, because these are not chemically bounded to the plastic matrix [7] and they have the ability of adsorbing toxic compounds from the environment such as heavy metals, persistent organic pollutants, etc. To compound the problem, the trophic transfer of microplastics in the trophic chain being able pose a threat on human health [8].

Several strategies based on pyrolysis–GC/MS [9,10], thermogravimetric analysis combined with gas chromatography coupled to mass spectrometry (TGA-GC/MS) [11,12], Raman spectroscopy [13–15], and FTIR-ATR spectroscopy [16–19] have been employed to analyze MPs in different environmental matrices. Other methodologies which incorporated microscopic analytical techniques and based on optical spectroscopy have been extensively applied for the detection, identification and characterization of plastic particles due to their relative low-cost, easiness, and time efficciency [20].

Although visual identification by optical microscopy helps to differentiate plastics from organic and mineral matter, it is still possible to underestimate or overestimate the quantity of plastics detected. For this reason, to date the results obtained by this technique are not adequate for the correct identification of MPs. To solve these problems, various studies have used different dyes such as red nile, rhodamine B, eosin B, hostasol yellow 3G or rose bengal for the identification of plastics by fluorescence [21–25].

A microscopic technique widely applied for the visual characterization of MPs is scanning electron microscopy (SEM). This method is used specifically for its ability to provide detailed information about the morphological structure of MPs, including precise details about their surface and particle size [26,27]. It has been used successfully to differentiate MPs between 1 μm and 1 mm [28]. But the current trend for the separation, identification and quantification of MPs is the combination of microscopic techniques with spectral analytical methods.

Spectroscopic analytical methods provide more precise information, enabling the identification of plastic particles and offering insights into the composition of the samples under study. FTIR-ATR microscopy has been used as a distinctive technique for identification of MPs since each polymer exhibits characteristic bands, because the vibrational energy levels are unique to each molecule.

Among the advantages of this technique are its speed, simplicity, and non-destructive nature [29–31]. In addition, FTIR-ATR is a very versatile technique that allows the study of samples of different characteristics, such as liquids, gels, fibers, films, etc. [32]. Besides, when plastic consists of a mixture of different polymers, its identification becomes challenging, even when a reference spectral library is used. Nevertheless, although the applicability of this technique has been outlined separately, the analytical protocols require the coordination of several methods to provide more accurate and reliable results. In this context, optical and/or SEM microscopy have also been applied complementarily in many cases to confirm the identification of the polymeric particles [33,34].

In this study, a combination of three analytical techniques such as FTIR-ATR, optical microscopy with staining, and SEM have been used complementarily to stablish an unequivocal protocol enabling the identification and differentiation of ten types of microplastics such as polyethylene (PE), PETE, LDPE, HDPE, PS, polycarbonate (PC), PP, PVC, polytetrafluoroethylene (PTFE), and polyamide (PA, Nylon 6,6).

2. Materials and methods

2.1. Plastic materials

The standards of PETE, LDPE, HDPE, and PS used for these studies were in pellet form (sized about 4 mm in diameter). Whereas the PVC and PE were in powder form. The aforementioned standards were purchased from Sigma Aldrich (Madrid, Spain). PC, PP, PTFE, and PA (Nylon 6,6) were in membrane form (with a diameter of 4.7 mm) were from Whatman (Little Chalfont, UK). To carry out the different characterization studies, the membranes were cut into square pieces with a size of 2 mm on each side.

2.2. Sample processing and FTIR-ATR spectra acquisition

FTIR analyses of the plastic materials used as references were carried out using the Attenuated Total Reflectance (ATR) mode. The ATR mode is characterized by its minimal preparation stages and the small amount of sample required, beside its effectiveness to obtain quality IR absorbance spectra. Infrared spectra were obtained using a Spectrum FT-IR-4100 Spectrometer equipped with ATR.

PRO ONE Accessory (FTIR-ATR) (JASCO, Tokyo, Japan) and Spectra Manager® Software Ver.2 (JASCO, Tokyo, Japan), in the medium infrared range between 4000 and 300 cm^{-1}, at resolution of 4 cm^{-1}, and with a data interval of 1 cm^{-1}. Measurements were carried out by placing the polymeric samples on the surface of the crystal (3.0 × 3.0 mm). Prior to each sample measurement, the FTIR-ATR crystal was cleaned with isopropanol. The obtained spectra for the different materials were compared with those in the

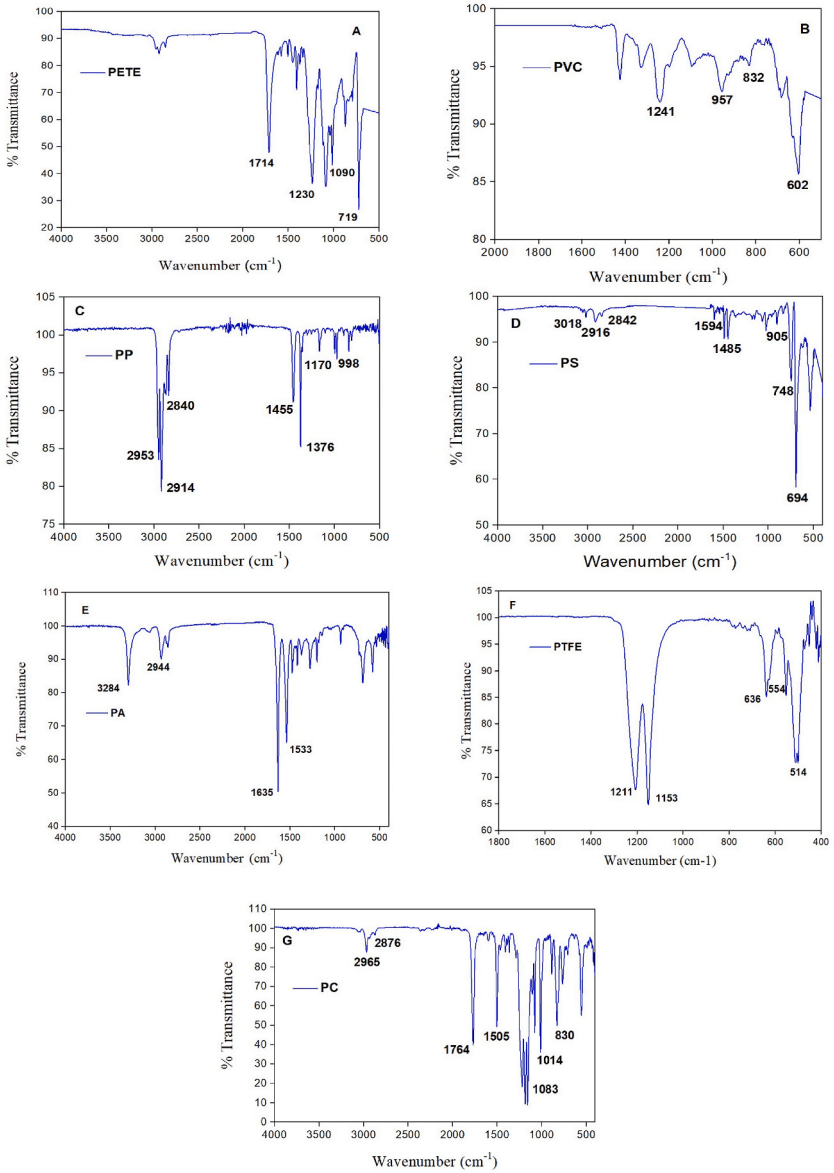

Fig. 1. Representative IR spectra obtained for plastic samples: (A) PETE, (B) PVC, (C) PP, (D) PS, (E) PA (Nylon 6,6), (F) PTFE and (G) PC.

equipment's library to confirm identification with certainty. In all cases, it was found that the matches between the obtained spectra and those in the library were above 90 %.

2.3. Staining procedure for optical microscopy study

Twelve different staining dye solutions (thorin, bromocresol green, bengal rose, lucifer yellow, alizarin, nile red, rodhamine B, titan yellow, black amide, phenol red, eriochrome blue, cresol red) were tested. Bromocresol green, alizarin, phenol red, titan yellow, cresol red, and eriochrome blue were supplied by Merck (Darmstadt, Germany). Thorin, bengal rose, lucifer yellow, nile red, rhodamine B, and black amide were obtained from sigma Aldrich (Madrid, Spain).

Staining dye solutions were prepared at 50 μg ml^{-1} in methanol (MACRON Fine Chemicals, Poland) because common plastics (most frequently used today) are resistant to this solvent [35]. The polymeric materials were placed in glass vials and exposed to 0.5 ml of different staining dye solutions for 1 h at room temperature and in the dark, following the procedure outlined by Maes et al., 2017 [21]. After that, polymers were dried at room temperature overnight [21]. Subsequently, the samples were placed in a sample holder to be observed by light microscope NIKON Eclipse 80i (Tokio, Japan) equipped with a monitor (Digital Sight DS-L1, Tokyo, Japan).

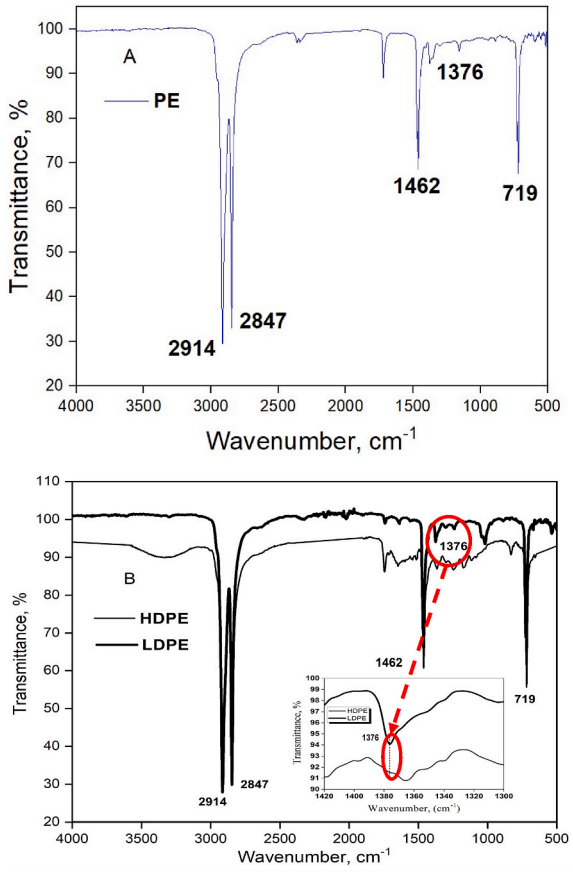

Fig. 2. IR *spectra* collected for *(A) PE, (B) HDPE* and LDPE.

2.4. Surface morphology analysis by scanning electron microscopy (SEM)

The surface morphology of the polymeric material was examined by a Scanning Electron Microscope (SEM)EM-30AX Plus COXEM from JASCO (COXEM, Korea). The samples were coated with Au using a SPT-20 sputter coater, step necessary before SEM analysis. The samples were mounted in a metal stub using a sticky carbon disc and they were coated with 50 nm of gold for 300 s at 50 mA. The prepared samples were then observed under SEM at an accelerated voltage of 20 kV and a magnification between 70 and 100,000 times.

3. Results and discussion

3.1. Identification of polymers by FTIR-ATR

To examine the differences between the studied plastic materials including PP, PE, HDPE, LDPE, PVC, PETE, PS, PC, PTFE, and PA (Nylon 6,6), FTIR-ATR spectra were performed. Figs. 1 and 2 show the corresponding IR spectra. The different main absorption bands for the ten polymeric materials studied were summarized in Table 1. The spectra were recorded and compared to absorption bands of each polymer reported in the literature [36–42]. The FTIR spectra of PETE (Fig. 1A), PP (Fig. 1C), PS (Fig. 1D), PA (Nylon 6,6) (Fig. 1E), PC (Fig. 1G), PE (Fig. 2A), HDPE (Fig. 2B), and LDPE (Fig. 2B) show medium to strong absorption bands around 3200–500 cm^{-1}. On the other hand, the bands in PVC (Fig. 1B) and PTFE (Fig. 1F), only are present around 1400-500 cm^{-1}. Spectra of PP and PS showed absorption bands around 3000–2800 cm^{-1} due to CH_2 asymmetric and symmetric stretch, but with different intensity. Additionally, a band present at 3284 cm^{-1} assigned to N–H stretch only is present in FTIR spectrum of PA (Nylon 6,6). PETE and PC are the only ones that show an intensity band around 1700 cm^{1}, which represents the group C–O stretch. In addition, PTFE is the sample with the fewest characteristic bands.

Fig. 2 shows the IR spectra obtained for PE (Fig. 2A), HDPE (Fig. 2B), and LDPE (Fig. 2B), respectively. We note that all three compounds show medium to strong absorption bands located around 719, 1462, 2847, and 2914 cm^{-1}. All of them showed strong adsorption bands around 2850-2915 cm^{-1} due to CH_2 symmetric and asymmetric stretch. Peaks located around 1462 and 719 cm^{-1} are assigned to CH_2 bend and C–O stretch, respectively. However, the greatest difficulty is to differentiate between HDPE and LDPE.

Table 1
Summary of important vibration modes and mode assignments for the FTIR-ATR spectra of the ten polymers identified.

Polymer	Absorption bands (cm^{-1})		Assignment	
PETE	1714	1090	C–O stretch	C–O stretch
	1230	719	C–O stretch	Aromatic ring C–H wag
HDPE	2914	1462	CH_2 asymmetric stretch	CH_2 bend
	2847	719	CH_2 symmetric stretch	CH_2 rock
PVC	1241	832	CH bend	C–C stretch
	957	602	CH_2 rock	C–Cl stretch
LDPE	2914	1376	CH_2 asymmetric stretch	CH_3 symmetric bend
	2847	719	CH_2 symmetric stretch	CH_2 rock
	1462		CH_2 bend	
PP	2953	1376	CH_3 asymmetric stretch	CH_3 symmetric bend
	2914	1170	CH_2 asymmetric stretch	CH bend, CH_3 rock and C–C stretch
	2840	998	CH_2 symmetric stretch	CH bend, CH_3 wag and CH_3 rock
	1455		CH_2 scissors	
PE	2914	1376	CH_2 asymmetric stretch	CH_3 symmetric bend
	2847	719	CH_2 symmetric stretch	CH_2 rock
	1462		CH_2 bend	
PS	3018	1485	Aromatic C–H stretch	Aromatic ring C–C stretch
	2916	905	CH_2 asymmetric and symmetric stretch	Aromatic C–H bend (out-of-plane)
	2842	748	CH_2 asymmetric and symmetric stretch	Aromatic C–H bend (out-of-plane)
	1594	694	Aromatic ring C–C stretch	Aromatic ring (out-of-plane) bend
PC	2965	1083	CH_3 asymmetric stretch	C–C stretch
	2876	1014	CH_3 symmetric stretch	Aromatic C–H (in-plane) bend
	1764	830	C–O stretch	Aromatic ring C–H (out-of-plane) wag
	1505		Aromatic ring stretch	
PTFE	1211	554	CF_2 symmetric stretch	CF_2 bend
	1153	514	CF_2 stretch	C–C–F bend
	636		C–C–F bend	
PA	3284	1635	N–H stretch	C–O stretch

because both compounds share the same structural unit, chemical bonds, functional groups, and identical wavenumbers [43]. When more in-depth studies of the FTIR spectra of HDPE and LDPE were carried out, it was observed a 1376 cm^{-1} band in the sample of LDPE, while in HDPE it only could be seen a small shoulder (Fig. 2B). These results are in accordance with those obtained by other authors. Asencio et al., 2009 [43] and Gulmine et al., 2002 [44] carried out studies where the band at 1376 cm^{-1} also allows the differentiation between HDPE and LDPE. Jung et al., 2018, developed a decision flow chart for differentiating HDPE, LDPE and linear low-density polyethylene (LLDPE) using FTIR-ATR spectra [37].

3.2. Optical microscopy and analyses of obtained images

The synthetic polymer samples stained with different dyes (thorin, bromocresol green, bengal rose, lucifer yellow, alizarin, nile red, rhodamine B, titan yellow, black amide, phenol red, eriochrome blue and cresol red) were observed under optical microscope to evaluate the polymer ability to adsorb the dye, which would allow to identify them.

Photographs of stained samples are shown in Fig. 3.

The identification of the type of polymer in MPs depends on the adsorption capacity towards the dye and the resulting appearance of the different polymers after this staining process. In general, the stained polymer samples exhibited varying colors and intensities when observed under the light microscope. The intense coloration that the samples acquired after the adsorption of the dyes tested was similar for certain polymeric materials (PP, PVC, PA (Nylon 6,6) and PTFE) but varied significantly in others, which exhibited less dye adsorption and therefore less degree of coloration (PETE, HDPE, LDPE, PS, PC and PE). PVC, PA (Nylon 6,6), PP and PTFE samples showed clear staining when thorin (dye 1) was used. This pattern across the results, with similar outcomes for bengal rose, titan yellow, and erichrome blue (dyes 2, 5 and 6), although PVC exhibited less intense staining in these cases. Nile Red (3) was also effective in staining the above-mentioned types of plastics in addition to PC. Rhodamine B (4) fully stained PP, PA (Nylon 6,6), and PTFE samples, while PETE, HDPE, PS, PC, and PVC samples showed only slight coloration. Similarly, bromocresol green, lucifer yellow, alizarin, amide black, phenol red and cresol red (dyes 7–12) were only capable of staining PVC, PP, PA (Nylon 6,6) and PTFE samples.

3.2.1. Scanning electron microscopy (SEM) results

To establish the surface morphology, physical characteristics (smooth, flat, porous, rough, etc.) of the microplastics of the different polymers, a SEM study was carried out. The results obtained are shown in Fig. 4. All tested microplastics exhibited different morphologies with characteristic surface textures and shapes. Under the electron microscope, the HDPE sample is the polymer that revealed greater smoothness and surface uniformity with a flat and smooth surface (Fig. 4A and B). In contrast, aggregates of irregular particles can be observed in PVC (Fig. 4E and F). The SEM photographs obtained for PS showed a representative pattern in the morphology of this polymeric material (Fig. 4I and J). In the case of PE (Fig. 4C and D), HDPE (Fig. 4G and H) and LDPE (Fig. 4K and L), respectively, less homogeneity can be observed in its surface compared to PETE. For these polymers that exhibit similar morphology,

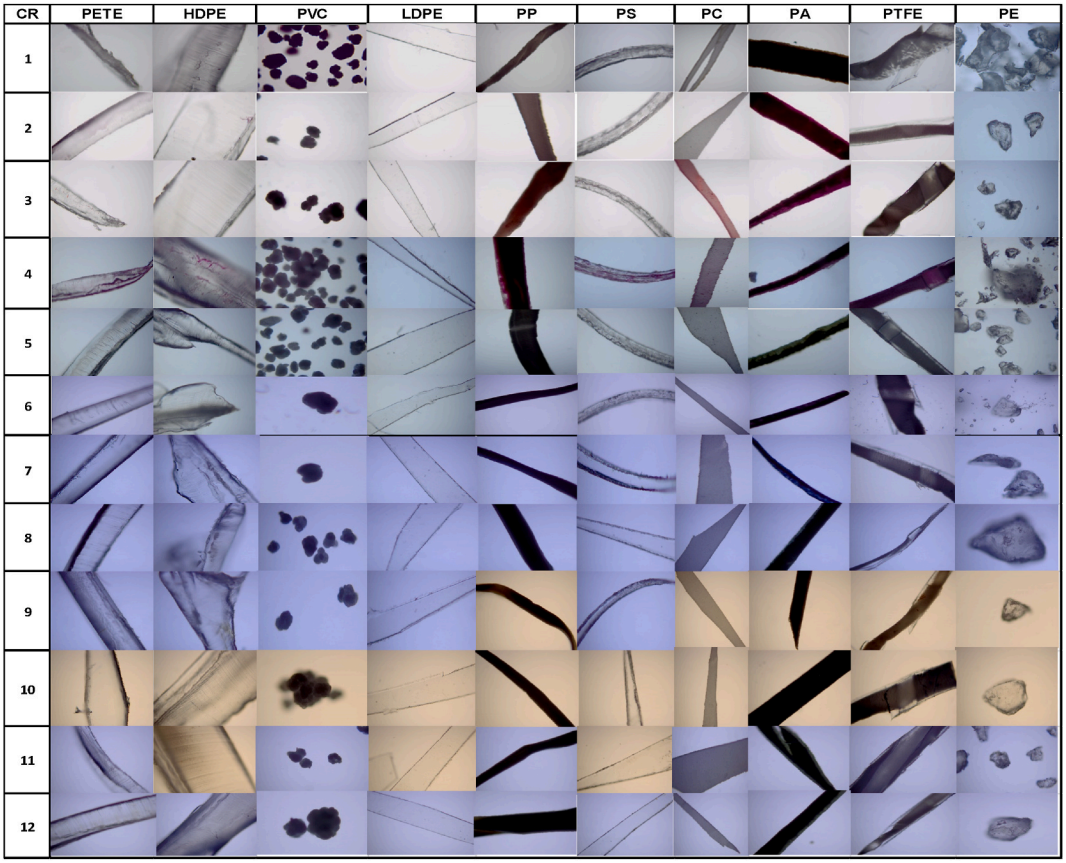

Fig. 3. Optical microscopy magnified images (objective 25x) observed under white light of the stained PETE, HDPE, PVC, LDPE, PP, PS, PC, PA (Nylon 6,6), PTFE and PE with different dyes: (1) thorin, (2) rose bengal, (3) nile red, (4) rhodamine B, (5) titan yellow, (6) eriochrome blue, (7) bromocresol green, (8) lucifer yellow, (9) alizarin, (10) amide black, (11) phenol red and (12) cresol red.

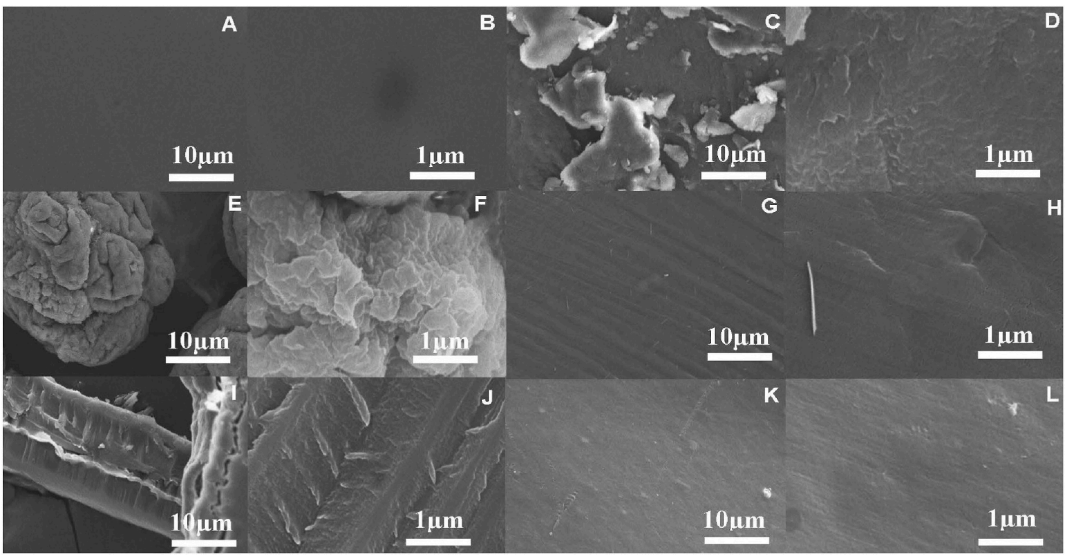

Fig. 4. SEM micrographs of the polymer sample's morphology: PETE (A) × 1K and (B) × 10K; PE (C) × 1K and (D) × 10K; PVC (E) × 1K and (F) × 10K; HDPE (G) × 1K and (H) × 10K; PS (I) × 1K and (J) × 10K; LDPE (K) × 1K and (L) × 10K

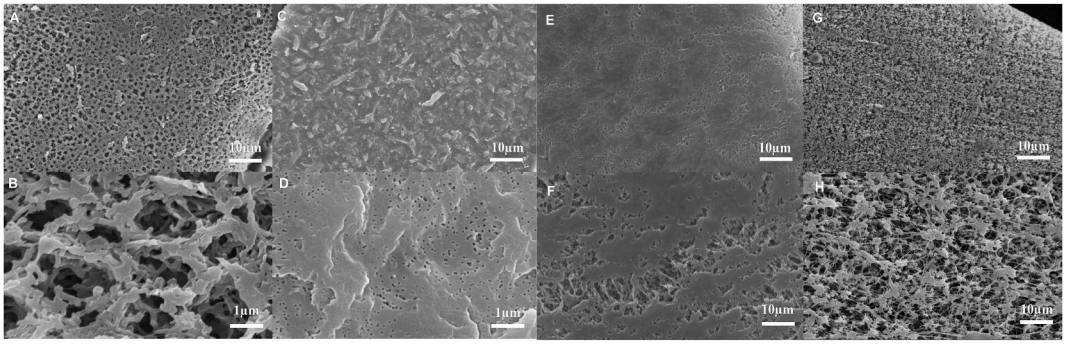

Fig. 5. SEM images for PA (Nylon 6,6) (A) × 1K and (B) × 10K; PC (C) × 1K and (D) × 20K; PP (E) × 1K and (F) × 5K; PTFE (G) × 1K and (H) × 5K

their differentiation by SEM is difficult.

However, SEM images of PA (Nylon 6,6) (Fig. 5A and B) revealed the presence of porous surfaces and cavities with a wide range of size distribution around 5 μm. Fig. 5 (C-D) shows the morphological surface of the PC, exhibiting a non-uniformly distributed porous structure with a mean diameter of 145.5 nm. In the case of PP, a microporous structure with slit-shaped pores was identified, with an average size range between 3 and 8 μm (Fig. 5E and F); while for PTFE a surface composed of nodes and cross-linked fibers with an average size of 3 μm is observed (Fig. 5G and H).

These results align with those obtained from the light microscopy studies, since polymers such as PETE, PE, HDPE, and LDPE, whose SEM images exhibited smoothness and flat uniformity on their surface, were not (or less) susceptible to adsorb staining solutions. In the same way, those MPs that showed porous structures by SEM analysis, such as PP, PA (Nylon 6,6), and PTFE were capable of adsorbing the dye solutions, acquiring a strong staining.

This fact implies that polymers can be unequivocally identified and classified into groups of MPs, those that are dyed (PA, PVC, PP, PTFE) and those that are not (PETE, PE, PC, HDPE, PS LDPE) with the dyes tested.

It is known that the adsorption of molecules on particle surfaces is generally due to hydrophobicity, electrostatics, van der Waals force, hydrogen bonding, which affect the extent to which dyes are adsorbed to the surfaces of microplastic particles [45,46]. These factors, in turn, are affected by pH, temperature, solvents, etc. [47]. According to Maes et al., the adsorption mainly depends on the degree of hydrophobicity between the dye and the polymer [21]. This statement is based on the partition coefficient, log Po which is defined as logarithm of the ratio of the concentration of a substance in 1-octanol at equilibrium and water at a specified temperature.

Magenau et al., (2015)[48] established the order of hydrophobicity of the polymers: PS > PETE > PP > PE > PVC > PA, meaning that the most hydrophobic polymers are the ones that adsorb the most [48]. Our results reveal that some polymers, despite having higher partition coefficients, do not adsorb dye. In the case of PETE, despite having a high partition coefficient (5.51), it does not adsorb any dye, which can be explained according to its less porous structure. In contrast, PA (1.85) and PVC (2.76) with lower coefficients, adsorb dyes and coincide with structures of higher porosity.

4. Conclusions

A systematic study with ten types of plastics materials standards (PETE, PE, HDPE, LDPE, PA (Nylon 6,6), PC, PP, PS, PVC and PTFE) were provided to establish a standardized protocol for their reliable identification and characterization by FTIR-ATR spectroscopy, scanning electron and optical microscopies. This study confirms the capacity of the FTIR technique for the identification of the different polymers tested from the unique vibrational modes that dictate the identity of the plastic in the resulting spectra obtained. The SEM images showed that PETE, PE, PVC, PS, HDPE, and LDPE exhibited smoothness and no porosity surfaces, while the surfaces of PP, PC, PTFE, and PA (Nylon 6,6) exhibited roughness and porosity. These results are supported and consistent with those obtained in the optical microscopy studies testing different dyes, where it can be observed how plastic materials with higher porosity (PP, PA (Nylon 6,6) and PTFE) are more prone to staining (thorin, bromocresol green, lucifer yellow, alizarin, amide black, phenol red). The Nile Red produced a marked staining in PVC, PP, PTFE, and PA (Nylon 6,6), and to a lesser extent in PC. This research demonstrated the significant potential of the combination of these three techniques for more accurate identification of MPs.

Data availability

All data generated or analyzed during this study are included in this published article.

CRediT authorship contribution statement

Dulce L. Soliz: Writing – original draft, Investigation, Funding acquisition, Data curation. **Gema Paniagua Gonza'lez:** Writing – review & editing, Supervision, Methodology, Investigation, Conceptualization. **Juan Munoz-Arnanz:** Writing – review & editing, Conceptualization. **Juan Carlos Bravo-Yagüe:** Writing – review & editing. **Pilar Fernandez Hernando:** Writing – review & editing,

Supervision, Project administration, Methodology, Funding acquisition. **Rosa María Garcinuno Martínez:** Writing – review & editing, Supervision, Funding acquisition, Conceptualization.

Declaration of competing interest

The authors declare that they have no known competing financial interests or personal relationships that could have appeared to influence the work reported in this paper.

Acknowledgements

This work was supported by the Community of Madrid (Spain) and European funding from FSE and FEDER Programs (project S2018/BAA-4393, AVANSECAL–II–CM), the Food and Agriculture Organization of the United Nations (FAO) and the National University of Distance Education (EUROPA INVESTIGACIÓN UNED—SANTANDER, ARTECAP, 2018-PUNED-0002; 096–044030, 2023-PUNED-0013; 50ANIV-GARCIN-UNED 50). This research has also been supported by a predoctoral contract funded by Banco Santander. This research was also financed by the Ministerio de Ciencia e Innovación Proyects (TED2021-131948A-I00, PlasThreat).

Authors would like to thank Dr. Paloma Collado Guirao for optical microscopy technical support.

References

[1] X. Chen, N. Yan, A brief overview of renewable plastics, Mater. Today Sustainability (2020) 7–8.
[2] N.N. Phuong, A. Zalouk-Vergnoux, L. Poirier, A. Kamari, A. Châtel, C. Mouneyrac, F. Lagarde, Is there any consistency between the microplastics found in the field and those used in laboratory experiments? Environ. Pollut. 211 (2016) 111–123.
[3] S.L. Wright, R.C. Thompson, T.S. Galloway, The physical impacts of microplastics on marine organisms: a review, Environ. Pollut. 178 (2013) 483–492.
[4] A. Sridhar, D. Kannan, A. Kapoor, S. Prabhakar, Extraction and detection methods of microplastics in Food and marine systems: a critical review, Chemosphere 286 (2022), https://doi.org/10.1016/j.chemosphere.2021.131653.
[5] C. Arthur, J. Baker, H. Bamford (Eds.), Proceedings of the International Research Workshop on the Occurrence, Effects, and Fate of Microplastic Marine Debris, NOAA Technical Memorandum NOS-OR&R-30, Sep 9-11, 2008, 2009. Sep 9-11, 2008.
[6] A.K. Amponsah, E.A. Afrifa, P.K. Essandoh, C.E. Enyoh, Evidence of microplastics accumulation in the gills and gastrointestinal tract of fishes from an estuarine system in Ghana, Heliyon 10 (2024) e25608, https://doi.org/10.1016/j.heliyon.2024.e25608.
[7] A. Parsaeimehr, C.M. Miller, G. Ozbay, Microplastics and their interactions with microbiota, Heliyon 9 (2023) e15104.
[8] H. Kye, J. Kim, S. Ju, J. Lee, C. Lim, Y. Yoon, Microplastics in water systems: a review of their impacts on the environment and their potential hazards, Heliyon 9 (2023) e14359.
[9] F. Lou, J. Wang, C. Sun, J. Song, W. Wang, Y. Pan, Q. Huang, J. Yan, Influence of interaction on accuracy of quantification of mixed microplastics using py-GC/MS, J. Environ. Chem. Eng. 10 (2022), https://doi.org/10.1016/j.jece.2022.108012.
[10] K. Chouchene, T. Nacci, F. Modugno, V. Castelvetro, M. Ksibi, Soil contamination by microplastics in relation to local agricultural development as revealed by FTIR, ICP-MS and pyrolysis-GC/MS, Environ. Pollut. 303 (2022), https://doi.org/10.1016/j.envpol.2022.119016.
[11] D. Sorolla-Rosario, J. Llorca-Porcel, M. Perez-Martínez, D. Lozano-Castello, A. Bueno-Lopez, Microplastics' analysis in water: easy handling of samples by a new thermal extraction desorption-gas chromatography-mass spectrometry (TED-GC/MS) methodology, Talanta 253 (2023), https://doi.org/10.1016/j.talanta.2022.123829.
[12] Y. Liu, R. Li, J. Yu, F. Ni, Y. Sheng, A. Scircle, J.V. Cizdziel, Y. Zhou, Separation and identification of microplastics in marine organisms by TGA-FTIR-GC/MS: a case study of mussels from coastal China, Environ. Pollut. 272 (2021), https://doi.org/10.1016/j.envpol.2020.115946.
[13] Y. Luo, C.T. Gibson, C. Chuah, Y. Tang, R. Naidu, C. Fang, Applying Raman imaging to capture and identify microplastics and nanoplastics in the garden, J. Hazard Mater. 426 (2022), https://doi.org/10.1016/j.jhazmat.2021.127788.
[14] H. De Frond, L. Thornton Hampton, S. Kotar, K. Gesulga, C. Matuch, W. Lao, S.B. Weisberg, C.S. Wong, C.M. Rochman, Monitoring microplastics in drinking water: an interlaboratory study to inform effective methods for quantifying and characterizing microplastics, Chemosphere 298 (2022), https://doi.org/10.1016/j.chemosphere.2022.134282.
[15] N. Jin, Y. Song, R. Ma, J. Li, G. Li, D. Zhang, Characterization and identification of microplastics using Raman spectroscopy coupled with multivariate analysis, Anal. Chim. Acta 1197 (2022), https://doi.org/10.1016/j.aca.2022.339519.
[16] J.L. Xu, K.V. Thomas, Z. Luo, A.A. Gowen, FTIR and Raman imaging for microplastics analysis: state of the art, challenges and prospects, TrAC, Trends Anal. Chem. 119 (2019).
[17] E. Uurasjarvi, E. Sainio, O. Setala, M. Lehtiniemi, A. Koistinen, Validation of an imaging FTIR spectroscopic method for analyzing microplastics ingestion by Finnish lake fish (Perca fluviatilis and Coregonus albula), Environ. Pollut. 288 (2021), https://doi.org/10.1016/j.envpol.2021.117780.
[18] A. Dilshad, M. Taneez, F. Younas, A. Jabeen, M.T. Rafiq, H. Fatimah, Microplastic pollution in the surface water and sediments from kallar kahar wetland, Pakistan: occurrence, distribution, and characterization by ATR-FTIR, Environ. Monit. Assess. 194 (2022), https://doi.org/10.1007/s10661-022-10171-z.
[19] P.S. Bauerlein, M.W. Erich, W.M.G.M. van Loon, S.M. Mintenig, A.A. Koelmans, A monitoring and data analysis method for microplastics in marine sediments, Mar. Environ. Res. (2022) 105804, https://doi.org/10.1016/j.marenvres.2022.105804.
[20] X. Luo, Z. Wang, L. Yang, T. Gao, Y. Zhang, A review of analytical methods and models used in atmospheric microplastic research, Sci. Total Environ. 828 (2022).
[21] T. Maes, R. Jessop, N. Wellner, K. Haupt, A.G. Mayes, A rapid-screening approach to detect and quantify microplastics based on fluorescent tagging with nile red, Sci. Rep. 7 (2017), https://doi.org/10.1038/srep44501.
[22] A.B. Labbe, C.R. Bagshaw, L. Uttal, Inexpensive adaptations of basic microscopes for the identification of microplastic contamination using polarization and nile red fluorescence detection, J. Chem. Educ. 97 (2020) 4026–4032, https://doi.org/10.1021/acs.jchemed.0c00518.
[23] F. Gbogbo, J.B. Takyi, M.K. Billah, J. Ewool, Analysis of microplastics in wetland samples from coastal Ghana using the rose bengal stain, Environ. Monit. Assess. 192 (2020), https://doi.org/10.1007/s10661-020-8175-8.
[24] H. Tong, Q. Jiang, X. Zhong, X. Hu, Rhodamine B dye staining for visualizing microplastics in laboratory-based studies, Environ. Sci. Pollut. Res. 28 (2021) 4209–4215, https://doi.org/10.1007/s11356-020-10801-4.
[25] V.C. Shruti, F. Pérez-Guevara, P.D. Roy, G. Kutralam-Muniasamy, Analyzing microplastics with nile red: emerging trends, challenges, and prospects, J. Hazard Mater. 423 (2022).
[26] A. Dąbrowska, M. Mielanczuk, M. Syczewski, The Raman spectroscopy and SEM/EDS investigation of the primary sources of microplastics from cosmetics available in Poland, Chemosphere 308 (2022), https://doi.org/10.1016/j.chemosphere.2022.136407.
[27] P. Samanta, S. Dey, D. Kundu, D. Dutta, R. Jambulkar, R. Mishra, A.R. Ghosh, S. Kumar, An insight on sampling, identification, quantification and characteristics of microplastics in solid wastes, Trends in Environmental Analytical Chemistry 36 (2022).
[28] C.B. Crawford, B. Quinn, Microplastic identification techniques, in: Microplastic Pollutants, Elsevier, 2017, pp. 219–267.

[29] V. Morgado, L. Gomes, R.J.N. Bettencourt da Silva, C. Palma, Validated spreadsheet for the identification of PE, PET, PP and PS microplastics by micro-ATR-FTIR spectra with known uncertainty, Talanta 234 (2021), https://doi.org/10.1016/j.talanta.2021.122624.
[30] R. Jaouani, C. Mouneyrac, A. Chatel, F. Amiard, M. Dellali, H. Beyrem, A. Michelet, F. Lagarde, Seasonal and spatial distribution of microplastics in sediments by FTIR imaging throughout a continuum lake - lagoon- beach from the Tunisian coast, Sci. Total Environ. 838 (2022), https://doi.org/10.1016/j.scitotenv.2022.156519.
[31] X. Yan, Z. Cao, A. Murphy, Y. Qiao, An ensemble machine learning method for microplastics identification with FTIR spectrum, J. Environ. Chem. Eng. 10 (2022), https://doi.org/10.1016/j.jece.2022.108130.
[32] J.C. Prata, J.P. da Costa, A.C. Duarte, T. Rocha-Santos, Methods for sampling and detection of microplastics in water and sediment: a critical review, TrAC Trends Anal. Chem. (Reference Ed.) 110 (2019) 150–159.
[33] W. Courtene-Jones, T. Maddalene, M.K. James, N.S. Smith, K. Youngblood, J.R. Jambeck, S. Earthrowl, D. Delvalle-Borrero, E. Penn, R.C. Thompson, Source, sea and sink—a holistic approach to understanding plastic pollution in the southern caribbean, Sci. Total Environ. 797 (2021), https://doi.org/10.1016/j.scitotenv.2021.149098.
[34] R. Perez-Reveron, J. Gonzalez-Salamo, C. Hernandez-Sanchez, M. Gonzalez-Pleiter, J. Hernandez-Borges, F.J. Díaz-Pena, Recycled wastewater as a potential source of microplastics in irrigated soils from an arid-insular territory (fuerteventura, Spain), Sci. Total Environ. 817 (2022), https://doi.org/10.1016/j.scitotenv.2021.152830.
[35] G. Erni-Cassola, M.I. Gibson, R.C. Thompson, J.A. Christie-Oleza, Lost, but found with nile red: a novel method for detecting and quantifying small microplastics (1 Mm to 20 Mm) in environmental samples, Environ. Sci. Technol. 51 (2017) 13641–13648, https://doi.org/10.1021/acs.est.7b04512.
[36] K.N. Fotopoulou, H.K. Karapanagioti, Surface properties of beached plastics, Environ. Sci. Pollut. Res. 22 (2015) 11022–11032, https://doi.org/10.1007/s11356-015-4332-y.
[37] M.R. Jung, F.D. Horgen, S.V. Orski, C.V. Rodriguez, K.L. Beers, G.H. Balazs, T.T. Jones, T.M. Work, K.C. Brignac, S.J. Royer, et al., Validation of ATR FT-IR to identify polymers of plastic marine debris, including those ingested by marine organisms, Mar. Pollut. Bull. 127 (2018) 704–716, https://doi.org/10.1016/j.marpolbul.2017.12.061.
[38] I. Noda, A.E. Dowrey, J.L. Haynes, C. Marcott, Group frequency assignments for mayor infrared bands observed in common synthetic polymers, in: J.E. Mark (Ed.), Physical Properties of Polymers Handbook, 2007, pp. 395–406.
[39] G. Mitchell, F. France, A. Nordon, P.L. Tang, L.T. Gibson, Assessment of historical polymers using attenuated total reflectance-fourier transform infra-red spectroscopy with principal component analysis, Herit Sci 1 (2013), https://doi.org/10.1186/2050-7445-1-28.
[40] S. Salmiati, Z. Yusop, N. Khoriha Eliysa Mohd Khori, T. Hadibarata, A combination of waste biomass activated carbon and Nylon nanofiber for removal of triclosan from aqueous solutions, J Environ Treat Tech 8 (2020) 1036–1045.
[41] S. Hisam, M. Taneez, M.Z. Sagheer, A. Dilshad, Microbeads in personal care products sold in Pakistan: extraction, quantification, characterization, and buoyancy analysis, Environ. Monit. Assess. 196 (2024), https://doi.org/10.1007/s10661-023-12227-0.
[42] S. Ramesh, K.H. Leen, K. Kumutha, A.K. Arof, FTIR studies of PVC/PMMA blend based polymer electrolytes, Spectrochim. Acta Mol. Biomol. Spectrosc. 66 (2007) 1237–1242, https://doi.org/10.1016/j.saa.2006.06.012.
[43] R. Chercoles Asensio, M. San Andres Moya, J.M. De La Roja, M. Gomez, Analytical characterization of polymers used in conservation and restoration by ATR-FTIR spectroscopy, Proceedings of the Anal BioanalChem 395 (December 2009) 2081–2096, https://doi.org/10.1007/s00216-009-3201-2.
[44] J.V. Gulmine, P.R. Janissek, H.M. Heise, L. Akcelrud, Test method polyethylene characterization by FTIR, Polym. Test. 21 (2002) 557–563, https://doi.org/10.1016/S0142-9418(01)00124-6.
[45] J. Bujdak, The effects of layered nanoparticles and their properties on the molecular aggregation of organic dyes, J. Photochem. Photobiol., C 35 (2018) 108–133.
[46] G. Giovannini, R.M. Rossi, L.F. Boesel, Changes in optical properties upon dye–clay interaction: experimental evaluation and applications, Nanomaterials 11 (2021) 1–16, https://doi.org/10.3390/nano11010197.
[47] J.N. Israelachvili, Intermolecular and Surface Forces, second ed., Academic Press, London, 1994.
[48] A.J.D. Magenau, J.A. Richards, M.A. Pasquinelli, D.A. Savin, R.T. Mathers, Systematic insights from medicinal chemistry to discern the nature of polymer hydrophobicity, Macromolecules 48 (2015) 7230–7236, https://doi.org/10.1021/acs.macromol.5b01758.